Journal of Molecular Graphics and Modelling 28 (2010) 834–841

Contents lists available at ScienceDirect

Journal of Molecular Graphics and Modelling

journal homepage: www.elsevier.com/locate/JMGM

Molecular dynamics investigation of cyclic natriuretic peptides: Dynamic properties reflect peptide activity

Elena Papaleo*, Laura Russo, Nasrin Shaikh, Laura Cipolla, Piercarlo Fantucci, Luca De Gioia

Department of Biotechnology and Biosciences, University of Milano-Bicocca, Piazza della Scienza 2, 20126 Milan, Italy

ARTICLE INFO

Article history:
Received 3 December 2009
Received in revised form 1 March 2010
Accepted 2 March 2010
Available online 7 March 2010

Keywords:
Cyclic peptide
Natriuretic peptide
Molecular dynamics
Free energy landscape
Dynamics and function conservation

ABSTRACT

Natriuretic peptides (NPs) are a family of structurally related hormone/paracrine factors (ANP, BNP and CNP), which mediate a broad array of physiological effects by interacting with specific guanylyl cyclase receptors (NPR) and have promising therapeutic and clinical applications. NPs are specific for different NPRs and share a common ring structure in which a disulfide bond between two conserved cysteine residues is formed. Residues within the cyclic loop are largely responsible for receptor selectivity. Structural features of free NPs in solution have not been investigated in details even if their characterization would be very useful in order to identify important aspects related to NPs function and receptor selectivity. In light of the above scenario, we carried out a 0.1 μs molecular dynamics investigation of NPs with the aim of providing a high-resolution atomistic view of specific of their conformational ensemble in solution. Our results clearly indicate that NP receptor-bound conformations are not stable solution structure and that induced-fit mechanisms are involved in the formation of NP-NPR complexes. Moreover, in agreement with the current view on strictly relationship between protein dynamics and protein function and activity, it turns out that differences in activity and NPR specificity of CNP and ANP/BNP might be correlated to different amino acid composition of the cyclic loop, propensity to form β-sheet structures, flexibility patterns, dynamics properties and free conformations explored during the simulations.

1. Introduction

Natriuretic peptides (NPs) are a family of structurally related hormone/paracrine factors. NPs mediate a diverse array of physiological effects ranging from blood pressure control to endochondral ossification [1,2]. This broad array of responses is achieved from the distinct actions of individual natriuretic peptides interacting with specific guanylyl cyclase receptors. Atrial natriuretic (ANP) and B-type natriuretic (BNP) peptides are secreted prevalently from the cardiac atria and ventricles, respectively. C-type natriuretic peptide (CNP) primarily stimulates long bone growth and its function is still not well understood. Moreover, a fourth class of NPs, the Dendroaspis natriuretic peptide (DNP), was isolated from the venom of *Dendroaspis angusticeps* [3,4].

The action of NPs is mediated through their cell-surface receptors, NPRs, which are a family of homologous single-transmembrane gylcosylated receptors (NPR-A, NPR-B, NPR-C). NPR-A and B transduce the NP signal through a large cytoplasmic domain with guanylyl cyclase activity [5,6]. ANP and BNP activate the transmembrane guanylyl cyclase NPR-A, whereas CNP activates the related cyclase NPR-B. A third natriuretic peptide receptor, natriuretic peptide receptor-C (NPR-C), clears natriuretic peptides from the circulation through receptor-mediated internalization and degradation. However, a signaling function for the receptor has been suggested as well [7–9]. Intriguingly, the C-terminal fragments generated by proteolysis of osteocrin (Ostn) are homologous to the NPs, specifically in the region matching the ring structure of the NPs, where the residues demonstrated to be essential for binding of NPs to their receptors are highly conserved [10]. Proteolytic Ostn fragments have been shown to selectively bind the NPR-C receptor, but not the guanylate cyclase receptors NPR-A and B [10,11].

Natriuretic peptides are also relevant for their potential therapeutic and clinical applications [2,12,13]. In fact, measurement of serum BNP levels is used as a diagnostic indicator for heart failure, and synthetic analogues of ANP and BNP have been approved for heart failure treatment [14,15]. Bifunctional chimeric natriuretic peptides have also been proposed as therapeutics [16,17].

From an evolutionary perspective, previous studies indicated that ANP and BNP evolved from CNP gene duplication events, suggesting that CNP is the most ancient family member [18]. From a structural perspective, NPs share a common ring structure of 17 amino acids, in which a disulfide bond between two conserved cysteine residues is formed. The common ring is generally accompanied by short head and tail segments, i.e., extensions from the amino acid carboxyl termini of the ring (Fig. 1A). Notably, exten-

* Corresponding author.
E-mail address: elena.papaleo@unimib.it (E. Papaleo).

1093-3263/$ – see front matter © 2010 Elsevier Inc. All rights reserved.
doi:10.1016/j.jmgm.2010.03.003

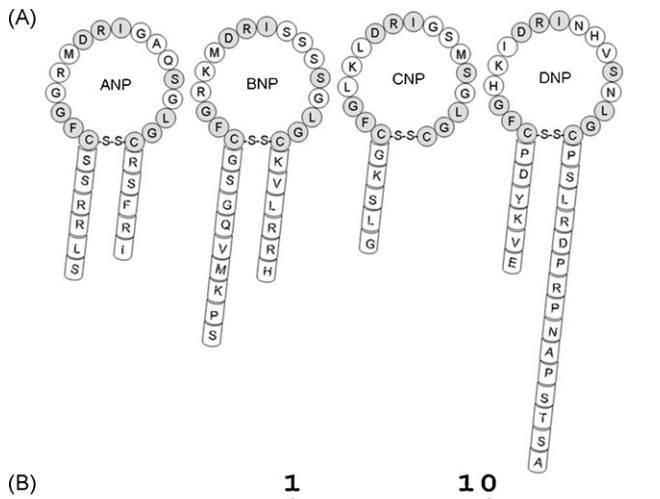

Fig. 1. Structure (A) and multiple sequence alignment (B) of NPs. The shaded circles indicate identical amino acids; each ring structure is stabilized by a disulphide bond. The multiple sequence alignment have been carried out by ClustalW2 (http://www.ebi.ac.uk/Tools/clustalw2). For sake of clarity, only the sequences of the cyclic portion of the NPs have been considered. Ostn-1 and Ostn-2 are the sequences of the C-terminal proteolytic fragments of the osteocrin peptide [10]. In order to highlight conserved regions, the alignment from Clustal W was submitted to ESpript [54].

sive structure-activity studies of NPs have converged on the idea that the residues within the cyclic loop are largely responsible for receptor selectivity, whereas the flanking residues outside the ring can modulate affinity [19,20].

Even if several crystal structures of NPRs in complex with NPs have been solved [21–24], a few structural data are available for free NPs [25,26]. The overall conformations of the three NPs in complex with NPRs feature a disk-like shape in an open, or extended conformations, with not remarkable stabilizing intramolecular interactions [23]. In fact, short peptides usually have no unique tertiary structure in solution, and it has been generally suggested that flexible hormones change from a solution ensemble of conformations to a single receptor-bound conformation [23,27].

Molecular dynamics (MD) simulations have been demonstrated to be a suitable technique to evaluate conformational ensemble of disordered peptides which consists of a variety of conformations [28–31]. In the this contribution, we present a molecular dynamics (MD) investigation of NPs in solution starting from their structure bound to the NPR-C [21,23] with the aim of providing a high-resolution atomistic view of their conformational ensemble in solution and of specific interactions that cannot be easily captured by experimental techniques [32–34].

2. Materials and methods

2.1. Molecular dynamics simulations

Molecular dynamics (MD) simulations were performer using the 3.3.3 version of the GROMACS software (www.gromacs.org), implemented on a parallel architecture with the GROMOS96 forcefield.

The X-ray structures of the natriuretic peptides ANP (pdb entry 1YK0 [23]), BNP (pdb entry 1YK1 [23]) and CNP (pdb entry 1JDP [23]) in complex with the receptor NPR-C were used as starting points for the MD simulations. In particular, only the atomic coordinates for the cyclic portion of the peptides were considered for the calculations.

The peptide structures were soaked in a triclinic box of SPC (Single Point Charge) water molecules and simulated using periodic boundary conditions. The box size was 57.8, 79.36, and 60.9 nm^3, containing 1817, 2559, 1925 SPC water molecules, in ANP, BNP and CNP, respectively. All the peptide atoms are at a distance equal or greater than 1.0 nm from the box edges. The ionization state of residues was set to be consistent with neutral pH and the tautomeric form of histidine residues was derived using GROMACS tools and confirmed by visual inspection.

Initially, the system was relaxed by molecular mechanics (steepest descent, 1000 steps). The optimization step was followed by 50 ps MD at 300 K (time step 1 fs) while restraining protein atomic positions using an harmonical potential. During equilibration the coupling constant to the external bath was set to 1 fs [35]. The system was slowly driven to the target temperature (300 K) and pressure (1 bar) through a series of short equilibration simulations.

Productive MD simulations were performed in the NPT ensemble at 300 K, using an external bath with a coupling constant of 0.1 ps. Pressure was kept constant (1 bar) by modifying box dimensions and the time-constant for pressure coupling was set to 1 ps [35]. The LINCS [36] algorithm was used to constrain bond lengths, allowing the use of a 2 fs time step. Electrostatic interactions were calculated using the Particle-mesh Ewald (PME) [37] summation scheme. Van der Waals and Coulomb interactions were truncated at 1.2 nm. The non-bonded pair list was updated every 10 steps and conformations were stored every 2 ps.

For ANP and CNP, a 100 ns simulation was carried out, whereas for BNP two 100 ns simulations (*replicas*) were carried out for each protein system, initializing the MD runs with different initial atomic velocities. In the following, the two MD trajectories collected for BNP but characterized by different initial velocities are referred to as *replica-1* and *replica-2*.

2.2. Analysis of molecular dynamics simulations

The root mean square deviation (rmsd), which is a crucial parameter in order to evaluate the equilibration of MD trajectories, was computed for mainchain atoms using the starting structure of the MD simulations as a reference. Conformations collected in the first 3 ns of simulations were discarded, in order to ensure that calculated parameters reflect the intrinsic properties of each system. For BNP, the equilibrated portions of each of the two *replicas* were joined together in a concatenated trajectory, which is representative of different directions of sampling around the starting structure.

The mainchain rmsd matrices have been computed by least square fitting on mainchain atoms on the equilibrated and concatenated trajectories. The rmsd matrices have been then processed using Gromos algorithm to extract clusters of similar conformations. Different rmsd cutoffs were tested and adopted for cluster analysis and a value of cutoff close to the average rmsd value derived from the rmsd matrices was selected (0.35 nm). The average structure of the cluster is defined as the peptide structure with the lowest average distance (rmsd) to all other structures belonging to the same cluster. Only clusters which collected at least 10% of the total structures were considered in order to filter out from the concatenated trajectory those structures which are not frequently sampled during the simulations.

The secondary structures were calculated using DSSP. The root mean square fluctuation (rmsf) per residue was calculated on

alpha-carbons (Cα), considering different sets of peptide conformations.

The hydrophobic interactions and hydrogen bonds have been calculated using routines implemented in PIC server [38]. The solvent accessible surface (SAS) was computed considering contribution of sidechain atoms and hydrophobic and hydrophilic contribution to the total SAS were calculated during the simulation time.

The visual analysis of protein structure was carried out using VMD (www.ks.uiuc.edu/Research/vmd) and Pymol (www.pymol.org).

2.3. Principal component analysis (PCA)

PCA reveals high-amplitude concerted motion in MD trajectories, through the eigenvectors (principal component) of the mass-weighted covariance matrix (C) of the atomic positional fluctuations [39]. In particular, all-atom C was calculated on the equilibrated portions of the trajectories and on the BNP concatenated trajectory:

$$C = cov(x) = \langle (x - \langle x \rangle)(x - \langle x \rangle)^{\mathrm{T}} \rangle$$

where $\langle\ \rangle$ indicates that average and x is the vector of the atomic positions.

After removal of the translational and rotational degrees of freedom (fitting each structure onto the initial one) the matrix C was calculated and diagonalized to obtain the eigenvectors and eigenvalues, which give information about correlated motions throughout the protein.

The dimensionality of the essential subspace was defined as the fraction of total motion described by the reduced subspace and it was computed as the sum of the eigenvalues relative to the included eigenvectors. This describes the amount of variance retained by the reduced representation of the total space.

A measure of the similarity of a MD trajectory to random diffusion is the cosine content (c_i) of the p_i principal component [40]:

$$c_i = \frac{2}{T}\left(\int cos(i\pi t)p_i(t)dt\right)^2 \left(\int p_i^2(t)dt\right)^{-1}$$

where T is the total simulation time. c_i is an absolute measure that can be extracted from covariance analysis and ranges between 0 (no cosine) and 1 (a perfect cosine). It has been demonstrated that insufficient sampling can lead to high c_i values, representative of random motions. The evaluation of the cosine contribution of the first eigen directions is sufficient to give a reliable idea of the protein behavior. When the cosine content of the first few principal components is close to 1, the largest scale motions in the protein dynamics resemble diffusion, and cannot be interpreted in terms of characteristic features of the energy landscape [41,42].

The overlap between the essential subspaces of different trajectories have been performed computing the root mean square inner product (rmsip) as a measure of similarity between subspaces defined by their basis vectors [43]:

$$\mathrm{RMSIP} = \frac{1}{D}\sum_{i=1}^{D}\sum_{j=1}^{D}(\eta_i^A \eta_j^B)$$

where η_i^A and η_i^B are the eigenvectors of the spaces to be compared and D the number of eigenvectors considered. Usually the rmsip is computed on the first 10 eigenvectors [44].

2.4. Free energy landscape (FEL)

The free energy landscape (FEL) of a protein can be obtained using a conformational sampling method that allows to explore the conformations near the native state structure [45]. Here, the MD simulations were adopted as a sampling technique. To achieve a two-dimensional representation of the FEL, we define the probability of finding the system in a particular state characterized by a value q_α of some variables of interest (*reaction coordinates*) as proportional to ($e^{-G\alpha/kT}$) where $G\alpha$ is the free energy of the state. The FEL can be obtained from:

$$G\alpha = -kT \ln\left[\frac{P(q_\alpha)}{P_{\max}(q)}\right]$$

where k is the Boltzmann constant, T is the temperature of simulation, $P(q_\alpha)$ is an estimate of the probability density function obtained from a histogram of the MD data and $P_{\max}(q)$ is the probability of the most probable state. Considering two different reaction coordinates q_i and q_j the two-dimensional free energy landscapes were obtained from the joint probability distributions $P(q_i, q_j)$ of the system.

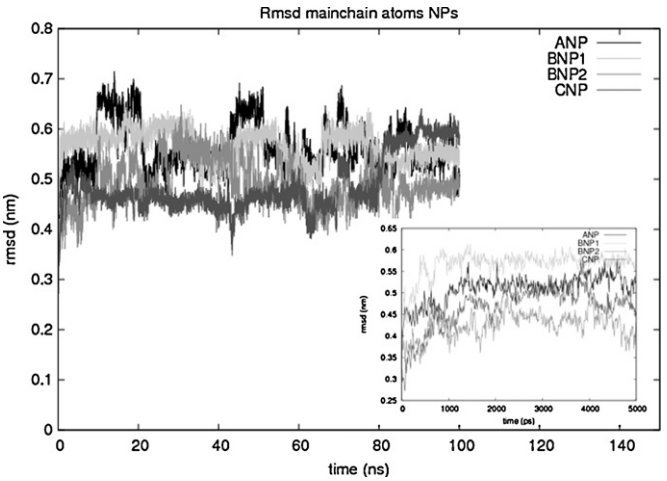

Fig. 2. Root mean square deviation (rmsd) of mainchain atoms. Rmsd is represented as a function of the simulation time for the different NP simulations. A zoom of the evolution of rmsd in the first 5 ns of simulations is shown in the lower panel.

3. Results

3.1. Evaluation of the conformational sampling in molecular dynamics (MD) simulations

Since MD simulations are necessarily limited in time, conformations visited are only a subset of all the possible conformations

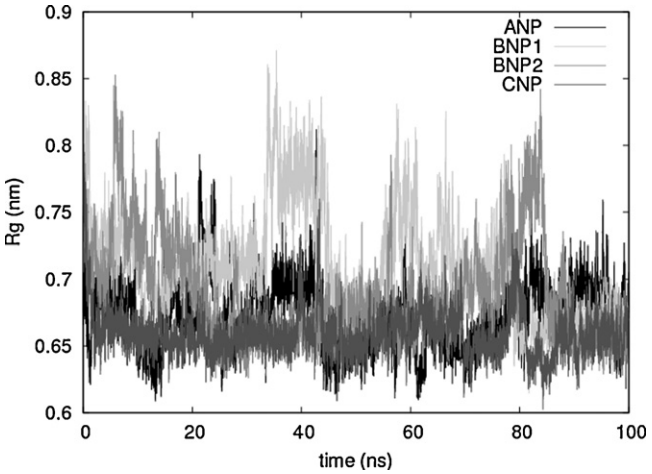

Fig. 3. Radius of gyration (Rg). The radius of gyration is shown as a function of the simulation time for the different NP simulations.

that the peptides can assume. In order to correlate the MD data with peptide characteristics, one should ensure a sufficiently high sampling efficiency. To this aim, the PCA analysis is a suitable tool to provide information about conformational sampling.

When the sampling of MD trajectories is insufficient, protein motions along the principal component appear indistinguishable from the dynamics of random diffusion, not allowing an accurate description of the free energy landscape. In particular, the first principal components of random diffusion resemble a cosine function and the sampling along these directions does not describe relevant motions. We calculated the cosine content of the first 20 principal components obtained from PCA of the single *replica*s and of the BNP concatenated trajectory (Fig. 1S, Supporting Information). The cosine content is generally low confirming that the collected MD simulations of NPs allow a reliable conformational sampling.

Therefore, in order to gain insights into the configurations visited by the system and to evaluate the conformational sampling, particular attention has been directed to the analysis of motions along the first eigenvectors. In fact, the first three eigenvectors are sufficient to describe a consistent part (more than 50%) of the total motion, and the subspace defined by them can be used as three-dimensional (3D) reference subspace to analyze protein

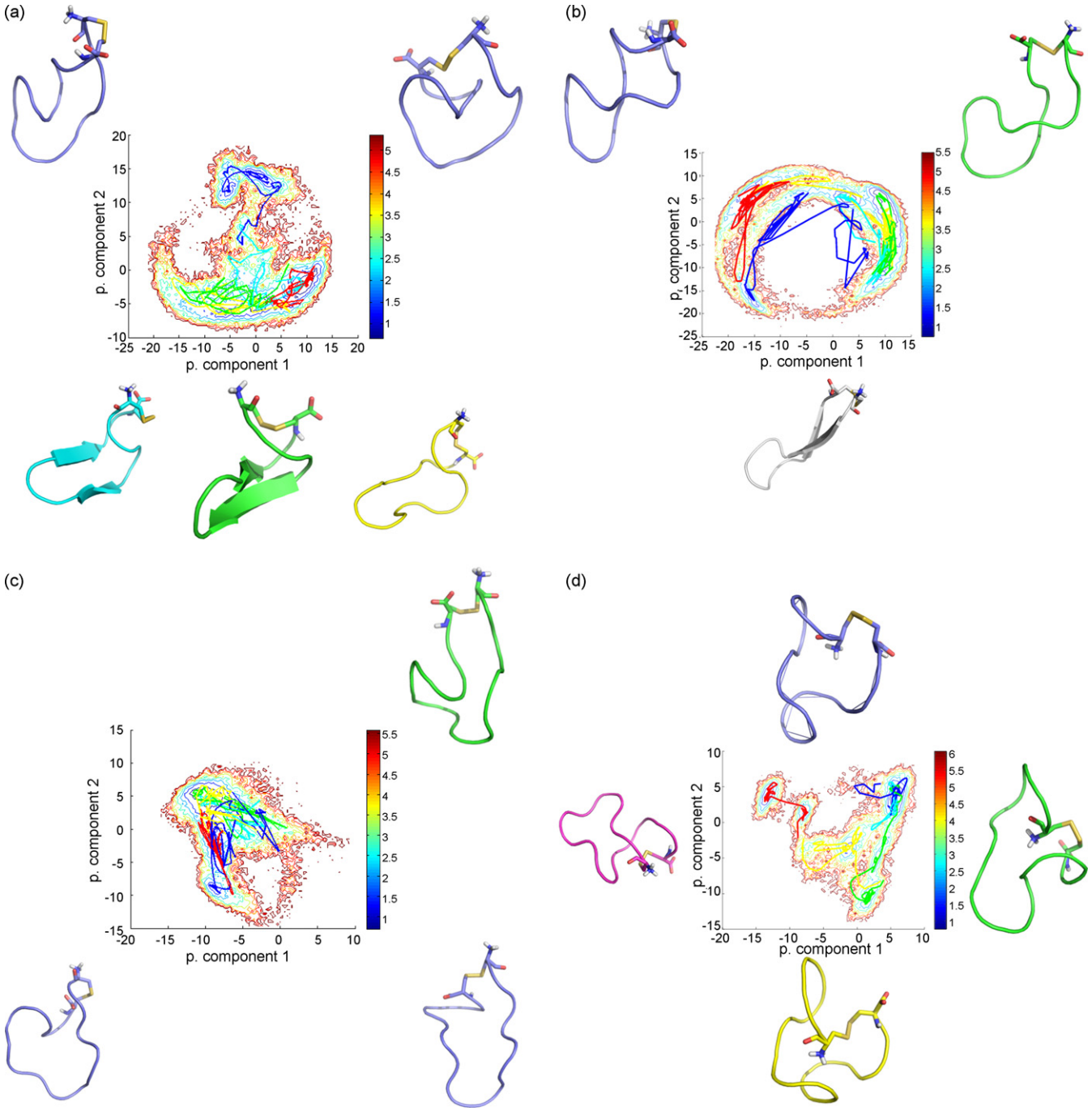

Fig. 4. Free energy landscape and average structures from cluster analysis. FEL using as reaction coordinates the projections of the ANP (A), BNP *replica-1* (B), BNP *replica-2* (C) and, CNP (D) trajectories along the 1st to 2nd principal components are shown. The free energy is given in kJ/mol and indicated by the color bar. Moreover, the trajectories explored by each single simulation are projected on the FEL and represented by a line colored from blue to red (from the initial to the last simulation frames). The average NP structures derived from cluster analysis and, corresponding to different minima on the FEL, are shown (see also Figs. 2S–5S).

dynamics. Indeed, the distribution of motion along the first three principal components tends to be anharmonic with two or more peaks, whereas on the later principal components the distribution tends to assume a narrow Gaussian shape (data not shown).

3.2. Conformational study of NPs in solution

Extensive structure-activity studies of NPs have converged on the idea that the residues within the cyclized loop are largely, responsible for receptor selectivity [1,2,19,20]. Therefore we focused on the analysis of the cyclic portion of the peptides, whose primary sequences present high similarity in the peptides (Fig. 1B). The differences in the primary sequences of the cyclic loop between ANP/BNP and CNP could reflect differences in the activity and specificity for different NPRs. The main differences between CNP and ANP/BNP clusterize in two regions of the ring (4–6 and 10–12).

The X-ray structure of NPs used as initial structure for MD simulations are derived by the complexes between the receptor NPR-C and the peptides. In fact, the structure of the free peptides rapidly diverged during MD simulations from the bound conformation, as one can see from rmsd analysis (Fig. 2) and radius of gyration (Rg) (Fig. 3) using as a reference structure the X-ray structure of NPs. The variability in the rmsd and Rg profiles over the simulation time also indicates that the conformations of the peptides are not stable in solution and might populate different substates.

Therefore, to better characterize the conformations assumed from the peptides in solutions, cluster analysis of mainchain rmsd matrices (Fig. 2S–5S, Supporting Information) and free energy landscape (FEL) analysis of the first principal components of PCA analysis were carried out (Fig. 4; Fig. 2S–5S, Supporting Information). Several minima on the FEL, which correspond to different structures, are populated during the simulations of the peptides, as can be observed by the presence of different structural clusters during the simulation time. From the FEL of BNP *replica-1* (Fig. 4B; Fig. 3S, Supporting Information) it seems that a region of the conformational landscape is not accessible to the peptide, therefore we carried out also a second *replica* (*replica-2*) for this peptide in order to improve the conformational sampling. The conformations sampled in *replica-2* present a certain degree of overlap with conformations sampled in *replica-1* and also allow to observe population of other substates which correspond to the empty space in the FEL of *replica-1*, as it turns out from the bidimensional projections along principal components 1 and 2 of the covariance matrix derived by the BNP concatenated trajectory (Fig. 6S, Supporting Information).

Moreover, the projection of the MD trajectories on the FEL and the analysis of the average structures of the clusters allow to better highlight conformational transitions between the FEL basins (Fig. 4). It turns out that several conformations are explored during the simulations of peptides and some of them populated the FEL basins whereas other are better described as metastable states allowing the conversion between a substate and another. It turns out that in ANP and BNP simulations transient formations of β-strand structures are observed, not present in CNP simulations and involving some of the residues conserved only in ANP and BNP

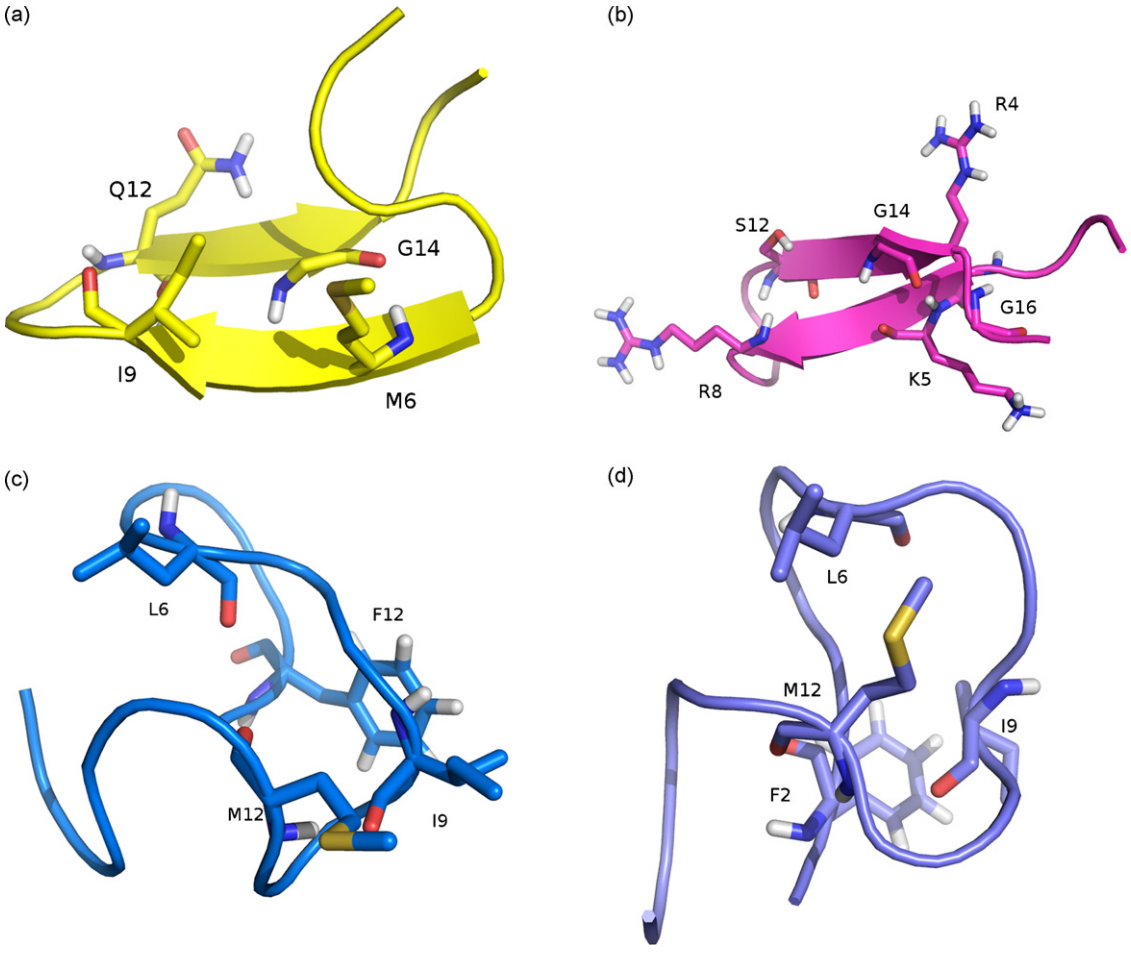

Fig. 5. Intramolecular interactions in NPs simulations. The residues involved in mainchain–mainchain H-bonds stabilizing the β-sheet structure in ANP (A) and BNP (B) simulations, as well as residues involved in a cluster of hydrophobic interactions in CNP (C and D) are shown as sticks. For sake of clarity, the residues involved in the most persistent intramolecular interactions during the simulations have been mapped on the 3D structures of reference structures extracted by the simulations.

(Fig. 1), as the polar residues at position 12, which is replaced by methionine in CNP. In particular two β-strands, involving the regions 5–9 and 12–16, and forming an antiparallel β-sheet are detectable in ANP and BNP simulations.

In order to provide a rational at the molecular level of the propensity of ANP and BNP to form a β-sheet structure, intramolecular interactions have been calculated on structures extracted from all the NPs simulations. It turns out that in ANP and BNP, the polar residues at position 12, interacting with residues at position 8 and 9, is crucial to maintain the correct pattern of mainchain–mainchain hydrogen bonds stabilizing the β-sheet (Fig. 5A and B). On the contrary, in CNP simulations the presence of a methionine at position 12 promotes the formation of a cluster of hydrophobic interactions, involving mainly residues 6, 9 and 2 (Fig. 5C and D).

The high conformational variability of the peptides is also confirmed by analysis of rmsf as flexibility index (Fig. 6; Fig. 7S, Supporting Information). The Cα rmsf per residue indicates the intensity of fluctuation of each residue with respect to the average structure. The average structure and consequently the rmsf profiles strongly depend from the simulation time considered, since considering different time intervals the average structure could change. Therefore, we calculated rmsf profiles on different time scales considering the flexibility over 100 or 10 ns (Fig. 7S, Supporting Information) and also considering successive sliding windows of 10 ns over the whole simulation time (Fig. 6). Coherently with the high conformational variability of the peptides, the rmsf profiles for each residue are characterized by significantly high values, indicating the absence of stable secondary structure elements. Moreover, the rmsf profiles of ANP (Fig. 6A) and BNP (Fig. 6B and C) present a higher similarity than rmsf profiles of CNP (Fig. 6D), suggesting that the dynamics of peptides with different specificity for NP receptors are strictly different.

In order to better characterized differences in protein dynamics of the CNP and ANP/BNP, rmsip has been calculated as a measure of subspace overlap (i.e. the overlap among sampled regions of the subspace). It allows comparison of the motions described by the first 10 principal components of each simulation. Rmsip ranges from 0 to 1: the value is 1 if sampled subspaces are identical, and 0 if the sampled subspaces are completely orthogonal. This parameter was calculated for all pairwise comparisons of NPs simulations (Fig. 7), confirming the previous analyses. CNP is characterized by lower rmsip values when compared to ANP and BNP simulations than rmsip values resulting from the comparison between ANP and BNP simulations. It turns out that the principal components describing the peptide motions present a low overlap between CNP and ANP/BNP whereas, ANP and BNP have more overlapping motions and conserved dynamic properties.

The similarity between ANP and BNP dynamics can be infer also from the analysis of the characteristics of the solvent accessible surface (SAS) of the sidechain atoms (Fig. 8). The average total SAS during the simulations of the three NPs is comparable, but their properties are strictly distinct: ANP and BNP are characterized by more hydrophilic residues exposed to the solvent and a less hydrophobic residues than CNP.

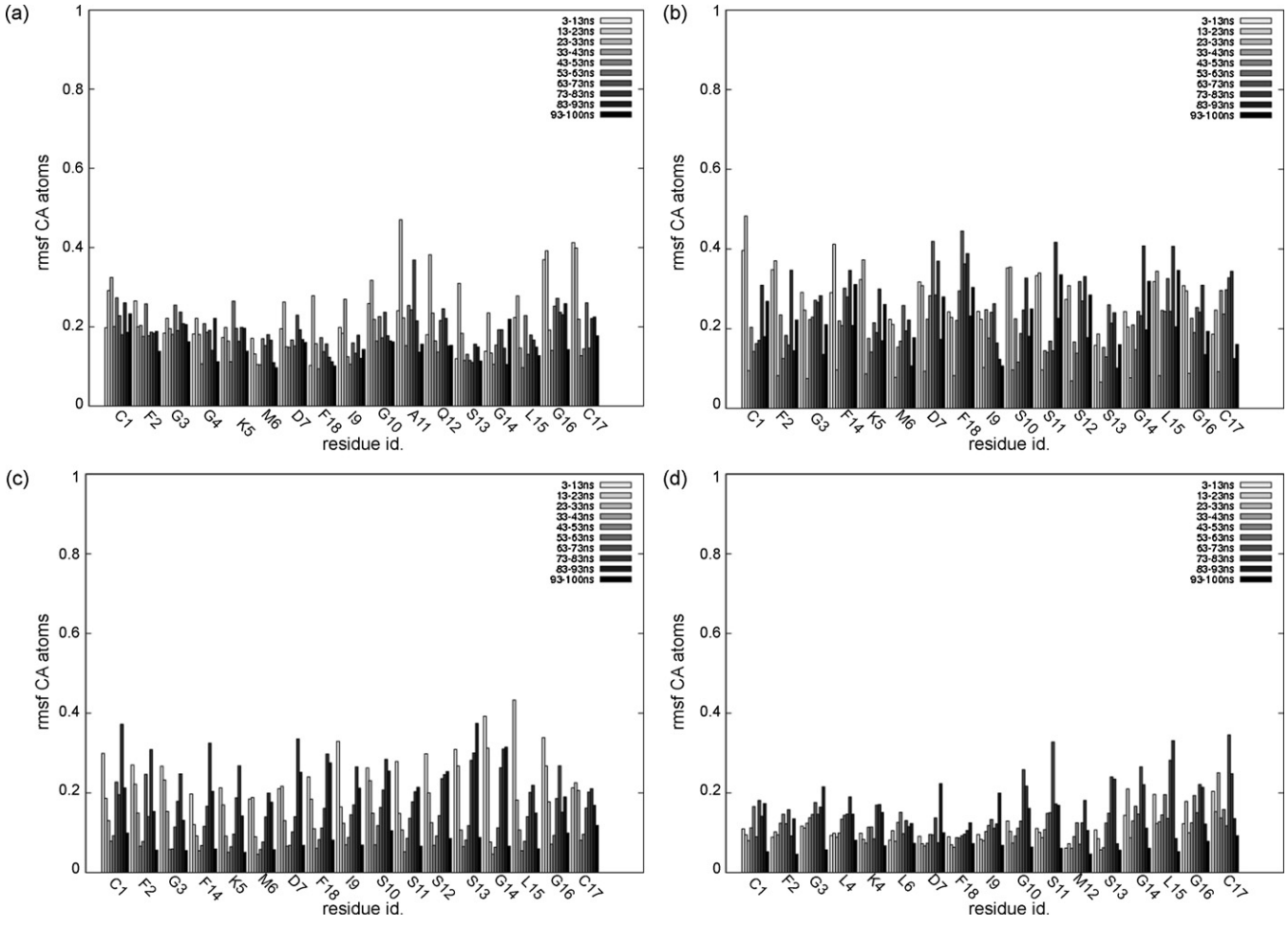

Fig. 6. Root mean square fluctuation (rmsf) as flexibility index. Cα rmsf per residue have been calculated considering sliding windows of 10 ns for the ANP (A), BNP *replica*-1 (B), BNP *replica*-2 (C) and, CNP (D) trajectories.

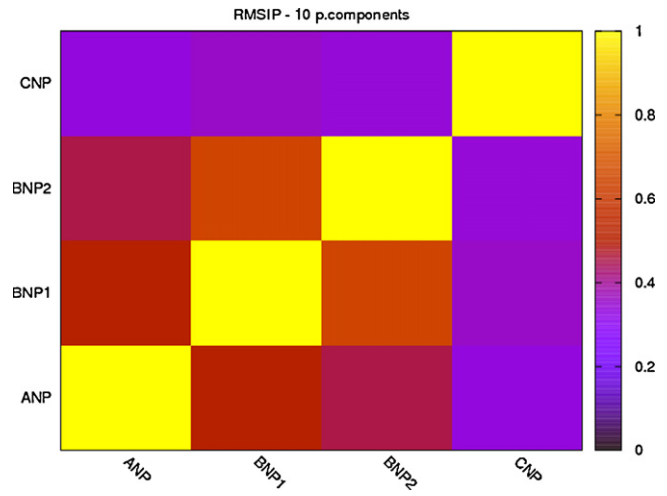

Fig. 7. Root mean square inner product (rmsip) as a overlap measure between conformational spaces explored during the simulations. The rmsip matrix shows with different shade of colors the rmsip values calculated comparing NPs simulations, considering the conformational subspace described by the first 10 principal components.

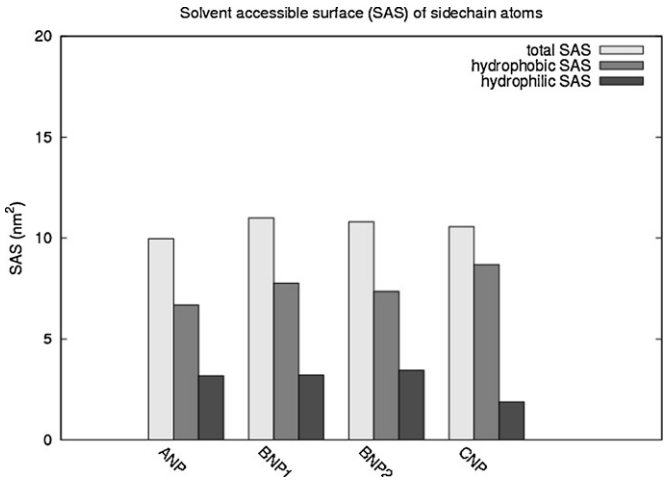

Fig. 8. Solvent accessible surface (SAS). The average total, hydrophilic and hydrophobic SAS calculated from the NPs simulations is shown.

4. Discussion

It has been suggested that rather than reflecting the receptor-bound structure, the conformations sampled by NPs in solution represent a compromise between the stability and flexibility necessary for potency, specificity and resistance to degradation [46]. In fact, the relatively high net charge and low mean hydrophobicity of NPs suggest that the hormone could be classified as being natively unfolded [46,47]. NPs could exploit intrinsic disorder for gaining high specificity coupled with low affinity, for allowing their binding to multiple partners because of structural plasticity, and for the creation of a large interface region with the dimeric receptor.

The MD investigation presented in this contribution reveals that NPs in solution are characterized by a great mobility, interconverting easily among a wide range of conformations. In the simulations, none NP structures which correspond to the bound conformations to the NPRs solved by X-ray crystallography [22–24] can be isolated showing that NP bound conformations are not stable solution structures. The result suggests that induced-fit mechanisms are involved in the formation of NP–NPR complexes, rather than conformational selection mechanisms. The intrinsic flexibility and conformational variability of NPs and induced-fit mechanisms upon binding to their specific receptor are very crucial data to consider for drug design and development of natriuretic peptide agonists or antagonists.

The present MD investigation also allows to raise other interesting points in the context of protein dynamics and its relevance for function. Protein flexibility and dynamics are widely acknowledged to be crucial for function [32,33,48–50]. The current view suggests that protein function is rooted in the energy landscape [33,48,50] and the fluctuations observed at equilibrium seem to govern biological functions. The striking correspondence between picosecond dynamics and longer scale conformational changes suggests that the physical origin of the catalytically important collective domain motions (microsecond to millisecond) is the fast-timescale (picosecond to nanosecond) local motions [48]. Differences in the fast fluctuations are encoded by differences in the amino acid sequence and influence the dynamics on picoseconds to nanosecond timescale and are ultimately connected to enzyme function. Moreover, backbone flexibility profiles diverge slowly, being conserved both at family and superfamily levels [50–52]. A recent study, in the context of cold adaptation, has shown that warm- and cold-adapted enzymes belonging to the same family present common dynamics signature related to the same fold but also peculiar differences which may reflect temperature adaptation [53].

In agreement with this current view on strictly relationship between protein dynamics and conservation of protein function and activity, it turns out, from our investigation, that differences in activity and NPR specificity of CNP and ANP/BNP seem to be correlated to different amino acid composition of the cyclic loop, different flexibility patterns, propensity to form β-sheet structure, dynamics properties and free conformations explored during the simulations. In particular, CNP is functionally distinct from other NPs, and has a high affinity to NPR-B, whereas other NPs prefer NPR-A. CD and FT-IR spectroscopy of porcine and rat BNP and ANP suggested that these peptides can exist under β-turn and β-mixed conformations, whereas porcine CNP exhibited not defined secondary structure [26]. Our simulations are in agreement with spectroscopic data and allow to clearly identify the regions of the ring which are involved in β-structure establishment, indicating that ANP/BNP amino acid residues not common to CNP are involved in stabilization of transient β-structures.

Acknowledgement

The authors thank CINECA (Project 696-2008) for the use of computational facilities.

Appendix A. Supplementary data

Supplementary data associated with this article can be found, in the online version, at doi:10.1016/j.jmgm.2010.03.003.

References

[1] L.R. Potter, S. Abbey-Hosch, D.M. Dickey, Natriuretic peptides, their receptors, and cyclic guanosine monophosphate-dependent signaling functions, Endocr. Rev. 27 (2006) 47–72.
[2] L.R. Potter, A.R. Yoder, D.R. Flora, L.K. Antos, D.M. Dickey, Natriuretic peptides: their structures, receptors, physiologic functions and therapeutic applications, Handb. Exp. Pharmacol. 191 (2009) 341–366.
[3] H. Schweitz, P. Vigne, D. Moinier, C. Frelin, M. Lazdunski, A new member of the natriuretic peptide family is present in the venom of the green mamba (*Dendroaspis angusticeps*), J. Biol. Chem. 267 (1992) 13928–13932.
[4] R. Barbouche, N. Marrakchi, P. Mansuelle, M. Krifi, E. Fenouillet, H. Rochat, M. El Ayeb, Novel anti-platelet aggregation polypeptides from Vipera lebetina venom: isolation and characterization, FEBS Lett. 392 (1996) 6–10.
[5] L.R. Potter, T. Hunter, Guanylyl cyclase-linked natriuretic peptide receptors: structure and regulation, J. Biol. Chem. 276 (2001) 6057–6060.

[6] M. Silberbach, C.T. Roberts, Natriuretic peptide signalling: molecular and cellular pathways to growth regulation, Cell Signal. 13 (2001) 221–231.
[7] M.B. Anand-Srivastava, Natriuretic peptide receptor-C signaling and regulation, Peptides 26 (2005) 1044–1059.
[8] R.A. Rose, N. Hatano, S. Ohya, Y. Imaizumi, W.R. Giles, C-type natriuretic peptide activates a non-selective cation current in acutely isolated rat cardiac fibroblasts via natriuretic peptide C receptor-mediated signalling, J. Physiol. 580 (2007) 255–274.
[9] R.A. Rose, W.R. Giles, Natriuretic peptide C receptor signalling in the heart and vasculature, J. Physiol. 586 (2008) 353–366.
[10] P. Moffatt, G.P. Thomas, Osteocrin—beyond just another bone protein? Cell. Mol. Life Sci. 66 (2009) 1135–1139.
[11] P. Moffatt, G.P. Thomas, K. Sellin, M. Bessette, F. Lafrenière, O. Akhouayri, R. St-Arnaud, C. Lanctôt, Osteocrin is a specific ligand of the natriuretic peptide clearance receptor that modulates bone growth, J. Biol. Chem. 282 (2007) 36454–36462.
[12] H. Chusho, N. Tamura, Y. Ogawa, A. Yasoda, M. Suda, T. Miyazawa, K. Nakamura, K. Nakao, T. Kurihara, Y. Komatsu, H. Itoh, K. Tanaka, Y. Saito, M. Katsuki, K. Nakao, Dwarfism and early death in mice lacking C-type natriuretic peptide, Proc. Natl. Acad. Sci. U.S.A. 98 (2001) 4016–4021.
[13] C.Y.W. Lee, J.C. Burnett, Natriuretic peptides and therapeutic applications, Heart Fail. Rev. 12 (2007) 131–142.
[14] D.G. Gardner, Natriuretic peptides: markers or modulators of cardiac hypertrophy? Trends Endocrinol. Metab. 14 (2003) 411–416.
[15] Y.H. Park, H.J. Park, B. Kim, E. Ha, K.H. Jung, S.H. Yoon, S.V. Yim, J. Chung, BNP as a marker of the heart failure in the treatment of imatinib mesylate, Cancer Lett. 243 (2006) 16–22.
[16] D.M. Dickey, J.C. Burnett, L.R. Potter, Novel bifunctional natriuretic peptides as potential therapeutics, J. Biol. Chem. 283 (2008) 35003–35009.
[17] O. Lisy, B.K. Huntley, D.J. McCormick, P.A. Kurlansky, J.C. Burnett, Design, synthesis, and actions of a novel chimeric natriuretic peptide: CD-NP, J Am. Coll. Cardiol. 52 (2008) 60–68.
[18] K. Inoue, K. Naruse, S. Yamagami, H. Mitani, N. Suzuki, Y. Takei, Four functionally distinct C-type natriuretic peptides found in fish reveal evolutionary history of the natriuretic peptide system, Proc. Natl. Acad. Sci. U.S.A. 100 (2003) 10079–10084.
[19] B.C. Cunningham, D.G. Lowe, B. Li, B.D. Bennett, J.A. Wells, Production of an atrial natriuretic peptide variant that is specific for type A receptor, EMBO J. 13 (1994) 2508–2515.
[20] J.R. Schoenfeld, P. Sehl, C. Quan, J.P. Burnier, D.G. Lowe, Agonist selectivity for three species of natriuretic peptide receptor-A, Mol. Pharmacol. 47 (1995) 172–180.
[21] X.I. He, D.C. Chow, M.M. Martick, K.C. Garcia, Allosteric activation of a spring-loaded natriuretic peptide receptor dimer by hormone, Science 293 (2001) 1657–1662.
[22] X. He, A. Dukkipati, X. Wang, K.C. Garcia, A new paradigm for hormone recognition and allosteric receptor activation revealed from structural studies of NPR-C, Peptides 26 (2005) 1035–1043.
[23] X. He, A. Dukkipati, K.C. Garcia, Structural determinants of natriuretic peptide receptor specificity and degeneracy, J. Mol. Biol. 361 (2006) 698–714.
[24] H. Ogawa, Y. Qiu, C.M. Ogata, K.S. Misono, Crystal structure of hormone-bound atrial natriuretic peptide receptor extracellular domain: rotation mechanism for transmembrane signal transduction, J. Biol. Chem. 279 (2004) 28625–28631.
[25] W.J. Fairbrother, R.S. McDowell, B.C. Cunningham, Solution conformation of an atrial natriuretic peptide variant selective for the type A receptor, Biochemistry 33 (1994) 8897–8904.
[26] M. Mimeault, A.D. Léan, M. Lafleur, D. Bonenfant, A. Fournier, Evaluation of conformational and binding characteristics of various natriuretic peptides and related analogs, Biochemistry 34 (1995) 955–964.
[27] V.N. Uversky, Natively unfolded proteins: a point where biology waits for physics, Protein Sci. 11 (2002) 739–756.
[28] T. Mittag, J.D. Forman-Kay, Atomic-level characterization of disordered protein ensembles, Curr. Opin. Struct. Biol. 17 (2007) 3–14.
[29] L.M. Espinoza-Fonseca, Leucine-rich hydrophobic clusters promote folding of the N-terminus of the intrinsically disordered transactivation domain of p53, FEBS Lett. 583 (2009) 556–560.
[30] A. Stavrakoudis, I.G. Tsoulos, Z.O. Shenkarev, T.V. Ovchinnikova, Molecular dynamics simulation of antimicrobial peptide arenicin-2: beta-hairpin stabilization by noncovalent interactions, Biopolymers 92 (2009) 143–155.
[31] E. Matyus, K. Blasko, J. Fidy, D.P. Tieleman, Structure and dynamics of the antifungal molecules Syringotoxin-B and Syringopeptin-25A from molecular dynamics simulation, Eur. Biophys. J. 37 (2008) 495–502.
[32] M. Karplus, J. Kuriyan, Molecular dynamics and protein function, Proc. Natl. Acad. Sci. U.S.A. 102 (2005) 6679–6685.
[33] K. Henzler-Wildman, D. Kern, Dynamic personalities of proteins, Nature 450 (2007) 964–972.
[34] G.G. Dodson, D.P. Lane, C.S. Verma, Molecular simulations of protein dynamics: new windows on mechanisms in biology, EMBO Rep. 9 (2008) 144–150.
[35] H.J.C. Berendsen, J.P.M. Postma, A. Di Nola, J.R. Haak, MD with coupling to an external bath, J. Phys. Chem. 81 (1984) 3684–3690.
[36] B. Hess, H. Bekker, H.J.C. Berendsen, J.G.E.M. Fraaije, LINCS: a linear constraint solver for molecular simulations, J. Comp. Chem. 18 (1997) 1463–1472.
[37] T. Darden, D.L. York, Pedersen Particle mesh Ewald: an N·log(N) method for Ewald sums in large systems, J. Chem. Phys. 98 (1981) 10089.
[38] K.G. Tina, R. Bhadra, N. Srinivasan, PIC: protein interactions calculator, Nucl. Acid Res. 35 (2007) W473–W476.
[39] A. Amadei, A.B. Linssen, H.J. Berendsen, Essential dynamics of proteins, Proteins 17 (1993) (1993) 412–425.
[40] B. Hess, Similarities between principal components of protein dynamics and random diffusion, Phys. Rev. E: Stat. Phys. Plasmas Fluids Relat. Interdiscip. Top. 62 (2000) 8438–8448.
[41] G.G. Maisuradze, D.M. Leitner, Free energy landscape of a biomolecule in dihedral principal component space: sampling convergence and correspondence between structures and minima, Proteins 67 (2007) 569–578.
[42] E. Papaleo, P. Mereghetti, P. Fantucci, R. Grandori, L. De Gioia, Free-energy landscape, principal component analysis, and structural clustering to identify representative conformations from molecular dynamics simulations: the myoglobin case, J. Mol. Graph. Model. 27 (2009) 889–899.
[43] A. Amadei, M.A. Ceruso, A. Di Nola, On the convergence of the conformational coordinates basis set obtained by the essential dynamics analysis of proteins' molecular dynamics simulations, Proteins 36 (1999) 419–424.
[44] H. Lei, C. Wu, H. Liu, Y. Duan, Folding free-energy landscape of villin headpiece subdomain from molecular dynamics simulations, Proc. Natl. Acad. Sci. U.S.A. 104 (2007) 4925–4930.
[45] M. Gruebele, Downhill protein folding: evolution meets physics, C. R. Biol. 328 (2005) 701–712.
[46] H. Peto, K. Stott, M. Sunde, R.W. Broadhurst, Backbone dynamics of oxidised and reduced forms of human atrial natriuretic peptide, J. Struct. Biol. 148 (2004) 214–225.
[47] D.L. Crimmins, J.L. Kao, The human cardiac hormone fragment N-terminal pro B-type natriuretic peptide is an intrinsically unstructured protein, Arch. Biochem. Biophys. 461 (2007) 242–246.
[48] K.A. Henzler-Wildman, M. Lei, V. Thai, S.J. Kerns, M. Karplus, D. Kern, A hierarchy of timescales in protein dynamics is linked to enzyme catalysis, Nature 450 (2007) 913–916.
[49] S. Maguid, S. Fernandez-Alberti, J. Echave, Evolutionary conservation of protein vibrational dynamics, Gene 422 (2008) 7–13.
[50] A.B. Law, E.J. Fuentes, A.L. Lee, Conservation of side-chain dynamics within a protein family, J. Am. Chem. Soc. 131 (2009) 6322–6323.
[51] S. Maguid, S. Fernández-Alberti, G. Parisi, J. Echave, Evolutionary conservation of protein backbone flexibility, J. Mol. Evol. 63 (2006) 448–457.
[52] A. Pandini, G. Mauri, A. Bordogna, L. Bonati, Detecting similarities among distant homologous proteins by comparison of domain flexibilities, Protein Eng. Des. Sel. 20 (2007) 285–299.
[53] E. Papaleo, M. Pasi, L. Riccardi, I. Sambi, P. Fantucci, L. De Gioia, Protein flexibility in psychrophilic and mesophilic trypsins. Evidence of evolutionary conservation of protein dynamics in trypsin-like serine-proteases, FEBS Lett. 582 (2008) 1008–1018.
[54] P. Gouet, E. Courcelle, D.I. Stuart, F. Métoz, ESPript: analysis of multiple sequence alignments in PostScript, Bioinformatics 15 (1999) 305–308.